Formation of stable hydrocarbon oil-in-water nanoemulsions by phase inversion composition method at elevated temperature

Soon Sik Kwon*, Bong Ju Kong*, Wan Goo Cho**,†, and Soo Nam Park*,†

*Department of Fine Chemistry, Cosmetic R&D Center, College of Energy and Biotechnology,
Seoul National University of Science and Technology, 232, Gongneung-ro, Nowon-gu, Seoul 137-743, Korea
**College of Medical Science, Jeonju University, 303, Cheonjam-ro, Wansan-gu, Jeonju 560-759, Korea

Abstract−Stable hydrocarbon oil (hexadecane, C16)/nonionic surfactant (HCO-60, Span 80)/water system oil-in-water nanoemulsions were prepared by the phase inversion composition method at elevated temperature. To minimize droplet size, the composition ratio for stable nanoemulsions, we experimented by changing the HLB value, oil/surfactant ratio, and droplet volume fraction. When the HLB_{mix} value 11, the nanoemulsions show a minimal sample droplet size of 360.3 nm. By varying the oil/surfactant ratio from 0.6 to 1.4, we found the optimum oil/surfactant ratio to be approximately 0.6, which corresponds to the minimum droplet size of 71.8 nm. We also varied the droplet volume fraction; when the droplet volume fraction is 0.06, the droplet size is very small. For the emulsion with the minimal droplet size, the polydispersity index is less than 0.3, which reflects a good monodispersity of the nanoemulsion. Viscosity and electrical conductivity measurements were carried out for determining the internal structure of the bicontinuous phase during the emulsification. When the water content ranges from 4 to 6 w/w%, the systems may have a bicontinuous or lamellar phase. Oil-in-water nanoemulsion stability assessment was performed by observing the droplet size as a function of storage time; we did not observe any change in droplet size over the course of a month.

Keywords: Nanoemulsions, Phase Inversion Composition Method, Ostwald Ripening, Bicontinuous, Long-term Stability

INTRODUCTION

Emulsion-based delivery systems are classified as emulsions, nanoemulsions, and microemulsions based on droplet size and thermodynamic kinetic stability [1-3]. Nanoemulsions are transparent or translucent systems because of small droplets, ranging from 20 to 150 nm. The Brownian motion of these small droplets prevents sedimentation or creaming; therefore, they exhibit increased kinetic stability, long-term stability, and the unique property of having no apparent flocculation or coalescence [4-6]. The ageing phenomenon of nanoemulsions is generally related to Ostwald ripening. Because of the Laplace pressure exerted on droplets, the smaller droplets tend to lose material in favor of bigger ones through diffusion into the dispersing phase [7,8]. It finally causes phase separation of nanoemulsions.

Typically, two main approaches are used for the preparation of nanoemulsions: high-energy and low-energy methods [9-11]. High-energy methods such as microfluidizers, high-pressure homogenizers, or ultrasound generators, utilize mechanical energy to break up macroscopic phases or to produce fine small droplets [12-14]. In contrast, low-energy methods utilize the chemical potential of the components or environmental conditions, which makes changes in the optimum curvature of surfactants by changing the temperature (at constant composition and phase inversion temperature;

PIT method) or the composition (at constant temperature and phase inversion composition; PIC method) [15-17]. These low-energy methods are advantageous (favorable) in terms of cost because they need no expensive equipment and are more energy efficient.

Nanoemulsification by phase inversion depends significantly on the structure of the phase from which the emulsification is performed. Sagitani et al. suggested that water content solubilized in the oil phase was a key factor [18]. Only if sufficient water content is solubilized can the oil phase be converted into an O/W nanoemulsion through the bicontinuous or lamellar phase [19-21].

We investigated the preparation of stable hydrocarbon oil (hexadecane)-in-water nanoemulsions by using a phase inversion composition method. We made an effort to find a minimal droplet size selection of a nanoemulsion system by varying the hydrophilic lipophilic balance (HLB) of the surfactant (with Span 80 and HCO-60), the oil/surfactant weight ratio, and the droplet volume fraction ($\varPhi$). In addition, we also did a study on the identification of the inversion point. The long-term stability of the nanoemulsion was evaluated by analyzing the droplet size, polydispersity index (PDI), and Ostwald ripening rate.

MATERIAL AND METHODS

1. Material

Hexadecane (C16, oil phase) was purchased from Aldrich-Sigma (USA). Nonionic surfactant of hydrogenated castor oil 60 (HCO-60) and sorbitane monooleate (Span 80, cosmetic grade) were obtained from Nikko Chemical Co. Ltd. (Tokyo, Japan) and Croda

†To whom correspondence should be addressed.
E-mail: snpark@seoultech.ac.kr, wgcho@jj.ac.kr

Chemicals, respectively. All reagents were used as received without further purification. Water was deionized and Milli-Q filtered.

2. Methods

2-1. Nanoemulsion Preparation

The surfactants (Span 80 and HCO-60) were dissolved into the oil phase, and then the surfactant-oil mixture and water phase were placed separately in a water bath at 85 °C. The water phase was added dropwise to the oil solution by the titration method. The experimental parameters were maintained at a constant value at a stirring rate of 300 rpm with a magnetic stirring and a water phase addition rate of 2 mL/min. After the emulsification, the samples were cooled to room temperature (~25 °C). The influence of nanoemulsion compositions, such as the HLB value, oil/surfactant ratio, and droplet volume fraction, was investigated.

2-2. Droplet Size and Polydispersity Index Analysis

Nanoemulsion droplet size and polydispersity index (PDI) were determined by dynamic light scattering (DLS Otsuka ELS-Z2, Otsuka Electronics, Japan) at a scattering angle of 165° utilizing an argon laser. Droplet measurements were carried out at room tempera-

ture. The particle size was measured without additional dilution, and an average value was determined by cumulative analysis and its distribution was resolved by use of the CONTIN method [22].

2-3. Phase Inversion Point

To observe the phase changes, viscosity and conductivity measurements were carried out for water content. In the case of viscosity, only if samples contained bubbles did we eliminate them by centrifuging (416, Labogene, Korea) and incubating in a water bath at 37 °C. Viscosity of the nanoemulsions was measured with DV-E and DV-II+ viscometers (RT, Brookfield, USA), and the measurements were carried out at room temperature and in the same container, by varying the spindle number and rotation speed (Table 1). Conductivity was measured by using a portable conductivity meter (COM-100, HM Digital Inc., Korea).
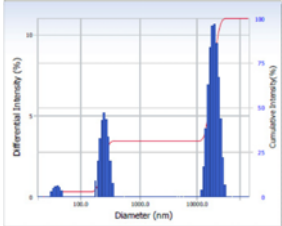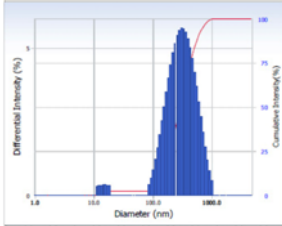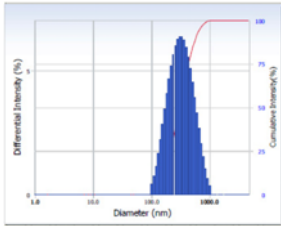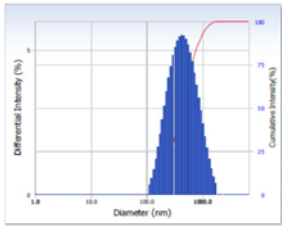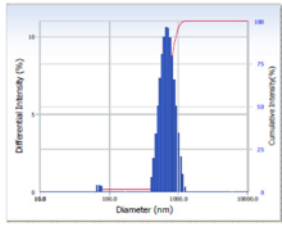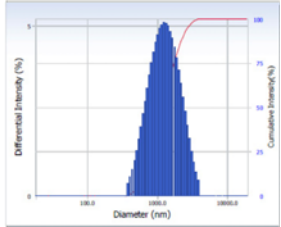
2-4. Long-term Stability Test

The long-term stability of the nanoemulsions was assessed by measuring the change in droplet size with storage time. The droplet size was determined at different time intervals (0, 4, 7, 11, 14, 18, and 21 days) by using dynamic light scattering. The samples

Table 1. According to water content, viscosity, and equipment

Equipment	DV-E viscometer					DV-II+Pro viscometer				
Water content (%)	4	5	6	8	10	2	15	20	40	60
Spindle number	96	96	96	96	95	63	62	61	61	61
Rate	6	2	2	6	60	6	50	100	100	100

Table 2. Droplet size and polydispersity index as a function of the HLB value for samples with O/S=1 : 1 and $\varphi=0.1$

HLB value	9.0	10.1	11.1
Intensity distribution			
Distribution results diameter (nm) std. dev	41.1±5.2 265.1±43.0 19,306.7±3,720.7	14.4±2.4 351.1±187.4	360.3±178.7
Polydispersity index	0.810	0.290	0.262
HLB value	12.1	13.0	14.0
Intensity distribution			
Distribution results Diameter (nm) std. dev	544.3±330.7	70.8±3.9 707.0±167.9	1,457.8±722.5
Polydispersity index	0.266	0.200	0.344

were kept sealed at room temperature.

2-5. Statistical Analysis

All experiments are repeated three times and statistical analysis was performed by Student's t-test.

RESULTS AND DISCUSSION

1. Optimization of the Nanoemulsions by the PIC Method at Elevated Temperature

1-1. Influence of the HLB Value

We examined the influence of the HLB value on nanoemulsion formation. The proper HLB value of the surfactants in the emulsion system was a key factor for the formation of minimal droplets [18]. This experiment was conducted by using a nonionic surfactant mixture consisting of Span 80 and HCO-60 emulsifier, which had HLB values of 4.5 and 14, respectively. The mixing ratios were regulated for minimal droplet size. The HLB values of the mixed emulsifiers were calculated by Eq. (1).

$$HLB_{mix}=HLB_A \times A\%+HLB_B \times B\%, \qquad (1)$$

where HLB_A, HLB_B, and HLB_{mix} are the HLB values of Span 80, HCO-60, and the mixed emulsifier, and A% and B% are the weight percentages of Span 80 and HCO-60 in the mixture, respectively. All the HLB values used were obtained at room temperature.

The HLB_{mix} influences the droplet size of nanoemulsions obtained by the PIC method [23,24]. The droplet size of the nanoemulsions

obtained by varying the mixed surfactant composition is shown in Table 2. Sample compositions of oil and surfactant mixture were fixed at 5 w/w%, respectively. The sum of the oil and surfactant mixture concentration is 10 w/w%. Especially, surfactant mixture consist of 1.5 w/w% Spna-80 and 3.5% HCO-60. According to Table 2, when the HLB_{mix} value has 11.1, it shows minimal sample droplet size of 360.3 nm, and in a range from 10 to 13, the PDI is less than 0.3, which reflects a good monodispersity of nanoemulsions. However, when the HLB_{mix} value was 9 or 14, we obtained unstable emulsions and saw creaming phenomenon as soon as cooling at room temperature occurred. Creaming phenomenon represented the unstable emulsion system that droplets float in the emulsion system. Therefore, we determined that in the following experiments the HLB_{mix} value the mixture of Span 80 and HCO-60 was fixed at 11.1, because of minimal droplet size at the HLB value.

1-2. Influence of the Oil/Surfactant Weight Ratio

The oil/surfactant weight ratio is the core element for stable nanoemulsion formation [9]. In a series of experiments, we investigated the influence of the oil/surfactant weight ratio on the droplet size and the PDI of the nanoemulsions, as presented in Table 3. The total weight of the surfactant mixture was kept constant at 5 w/w% (Span 80 [1.5 w/w%]+HCO-60 [3.5 w/w%], HLB value was fixed at 11.1), and the oil phase was varied (range of 3-7 w/w%). We observed that each droplet size increased from 76.7 to 579.9 nm when the oil/surfactant weight ratio increased from 0.6 to 1.4, respectively. The PDI is less than 0.3, which reflects a good monodisper-

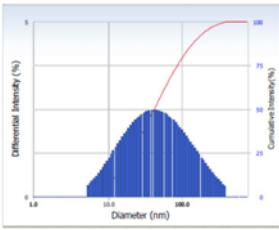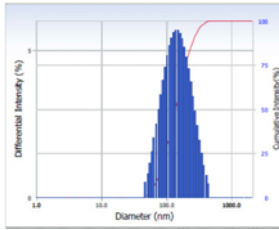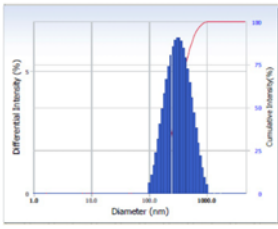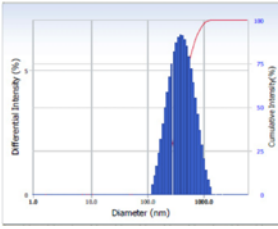**Table 3. Droplet size and polydispersity index as a function of the oil/surfactant weight ratio with HLB value=11**
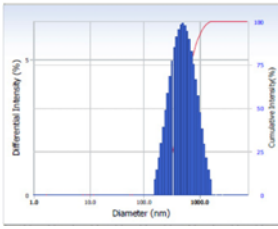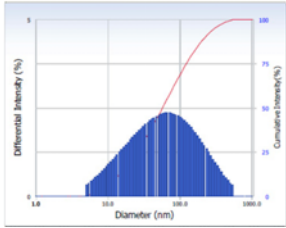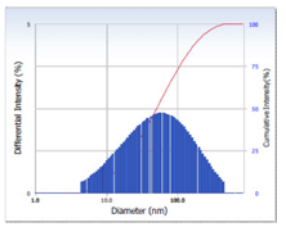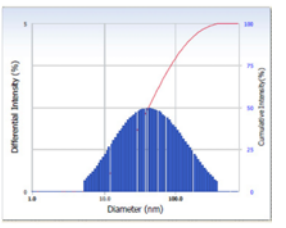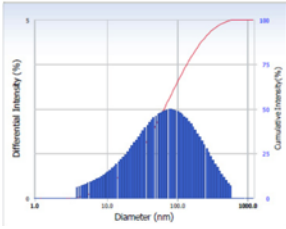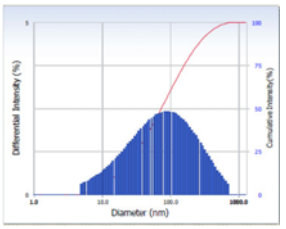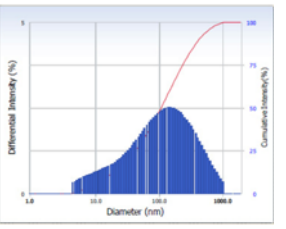
Oil/Surfactant weight ratio	0.6		0.8	
Intensity distribution				
Distribution results diameter (nm) std. dev	71.8±73.1		163.5±81.0	
Polydispersity index	0.281		0.223	
Oil/Surfactant weight ratio	1.0	1.2		1.4
Intensity distribution				
Distribution results diameter (nm) std. dev	360.3±178.7	468.2±238.1		579.9±303.3
Polydispersity index	0.262	0.235		0.246

Table 4. Droplet size and polydispersity index as a function of the droplet volume fraction (Φ) value with HLB value=11 and O/S=0.6

Droplet volume fraction	0.06	0.07	0.08
Intensity distribution			
Distribution results diameter (nm) std. dev	93.8±87.8	87.2±79.6	76.8±73.1
Polydispersity index	0.321	0.333	0.282
HLB value	0.10	0.12	0.16
Intensity distribution			
Distribution results diameter (nm) std. dev	107.3±99.4	125.3±112.8	182.5±173.5
Polydispersity index	0.329	0.335	0.378

sity of nanoemulsions. Also, emulsion turbidity is more transparent as the oil/surfactant weight ratio decreases. Based on the above result, we can conclude that a relatively higher surfactant concentration in the oil/surfactant mixture makes the droplet size smaller. In other words, droplet size decreases when the surfactant concentration increases. The high surfactant concentration increases the stability of the system because an excess of surfactant in the system is necessary to stabilize the interface of the oil droplets against coalescence during emulsification [25]. In addition, nanoemulsion droplet size was increased by reducing surfactant/water ratio at a fixed oil ratio or by increasing the oil/water ratio at a fixed surfactant ratio [26].

1-3. Influence of Droplet Volume Fraction (Φ)

In high-energy methods, when the range of the droplet volume fraction is from 0 to 0.6 ($0<\Phi\leq0.6$), stable nanoemulsions that will monodisperse can generally be formed. The size distribution of these emulsions did not change over a month [12]. In contrast, in low-energy methods, most nanoemulsions are prepared at relatively low volume fractions of the dispersed phase ($0<\Phi\leq0.2$) [15]. The effect of the droplet volume fraction on droplet size distribution has been studied less frequently because of the disadvantage of storage stability, especially when the droplets are concentrated [9].

In the droplet volume fraction experiment, we reduced the addition amount of the water phase, not the inner phase, to control the droplet volume fraction. Once oil droplets were formed, the water was added only as a diluent. The droplet size is governed by the structure of the bicontinuous phase [27]. Other parameters of the
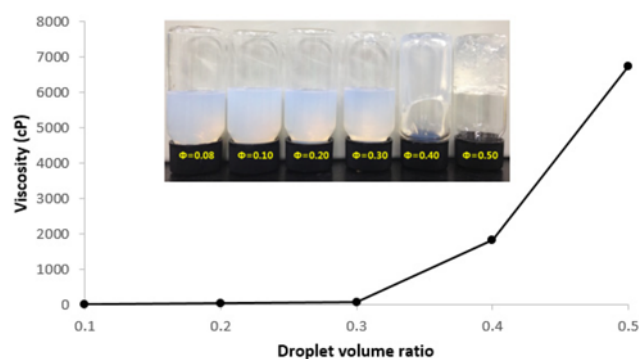

Fig. 1. Viscosity as a function of the droplet volume fraction with HLB value=11, O/S=0.6.

HLB value and the oil/surfactant ratio were fixed at 11.1 and 0.6, respectively. The droplet volume fraction, given by the oil volume fraction plus the surfactant volume fraction, varied from 0.06 to 0.16 (Table 4). The droplet size increased with the increase of the droplet volume fraction. However, the viscosity also increased as the inner ratio increased. When the inner volume fraction was approximately 0.5, the viscosity of the nanoemulsion dramatically increased (Fig. 1). It is considered to be a phenomenon caused by the formation of a liquid lamellar phase rather than inner phase interaction or formation of tumbling clusters [28].

2. Phase Inversion Point

As stated above, we determined the minimal droplet size com-

position of the nanoemulsion. We obtained the minimal droplet size composition with droplet size below 100 nm, which is only the HLB value (11.1), the oil/surfactant weight (0.6), and droplet volume fraction (0.08), respectively.

The phase inversion composition (PIC) mechanism by the low-energy method follows below. The water phase was added drop-wise to the oil phase. First, these systems form a W/O emulsion. With adding of the water phase, the W/O emulsion is converted to the bicontinuous or lamellar phase. Through these pathways, it finally forms the O/W emulsion with smaller oil droplets (nano size) upon further increase of the water content [21].

Typically, viscosity and electrical conductivity measurements were confined to the internal structure region of the bicontinuous
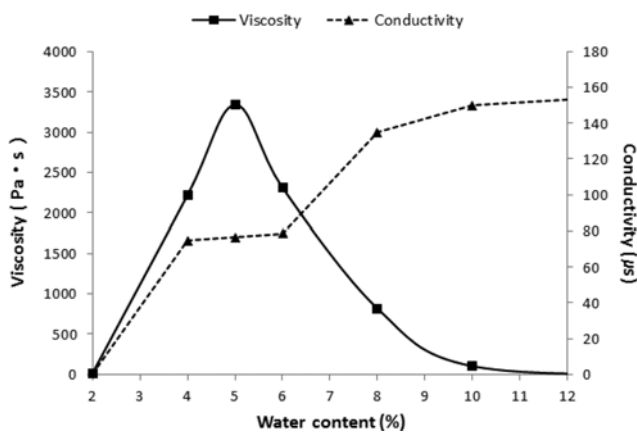

Fig. 2. Viscosity (■) and conductivity (▲) as a function of the increasing water content (%) with HLB value=11, O/S=0.6, and droplet volume fraction=0.08.

or lamellar phase [29-31]. The results of viscosity and electrical conductivity are shown in Fig. 2. Depending on water content, viscosity gradually increased from 0% to 5%, and then 5% water content reached maximum value, and further water content decreased viscosity. At the maximum value, we observed a gel-like formation, which indicated that they formed the bicontinuous or lamellar phase at 5% water content. To demonstrate the bicontinuous or lamellar phase, a further experiment was performed by use of electrical conductivity (Fig. 2). Adding the water content was followed by a linear conductivity increase from 0% to 4%. When a water content of 4%-6% is reached, conductivity tends toward a constant value. This result indicated that the structure of the system changes from W/O emulsion to bicontinuous structure and/or multiple emulsions with a high disperse phase volume fraction [26,32]. Above 6% water content, conductivity gradually increases when water is added. This development means that bicontinuous structures convert to the O/W emulsion. By using viscosity and electrical conductivity measurements, we can confirm the phase inversion point. Consequently, a water content range of 0%-4% may have W/O emulsions, and further water content, in the range of 4%-6%, may have a bicontinuous or lamellar phase. Above 6% water content, this system forms the O/W emulsion. According to the comprehensive experimental results of Section 3, and Section 4, schematic phase behavior of a ternary system is shown in Fig. 3.

3. Long-term Stability

The irreversible droplet size increase of nanoemulsions arises by two main mechanisms: coalescence and Ostwald ripening. First, coalescence is caused by the collision of different droplets. Consequently, droplets rupture and merge into one large droplet, and the droplet size gradually increases. If coalescence is the driving force behind instability of nanoemulsions, the change of droplet
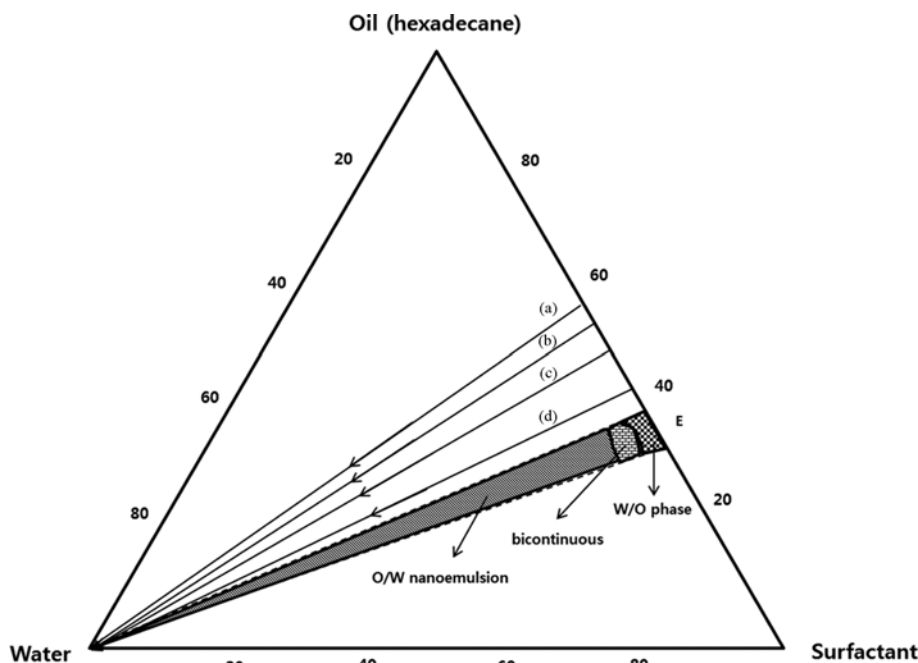

Fig. 3. Schematic phase behavior of ternary water/nonionic surfactant mixture/hexadecane oil systems. HLB value was fixed at 11. (a) O/S ratio=1.4, (b) O/S ratio=1.2, (c) O/S ratio=1.0, (d) O/S ratio=0.8, (e) O/S ratio=0.6.
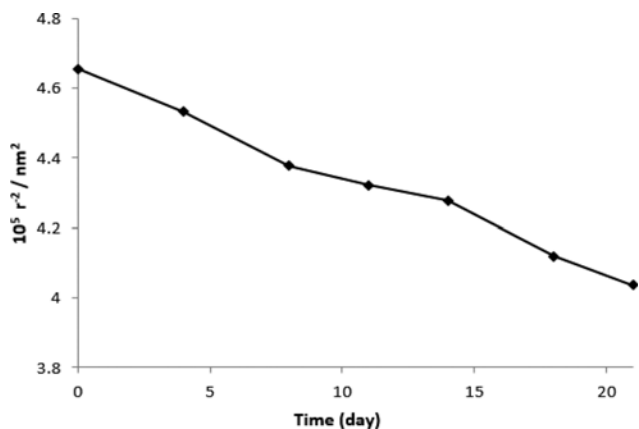
Fig. 4. The r^{-2} of nanoemulsion as a function of time for samples with HLB value=11, O/S=0.6, and droplet volume fraction= 0.08.

size with time may follow Eq. (2).

$$1/r^2=1/r_0^2-8\pi/3\,Ft, \tag{2}$$

where r is the average droplet radius after time t, r_0 is the value at t=0, and F is the frequency of ruptures per unit on the surface of the film. Although Eq. (2) was developed for concentrated systems, we used it to confirm the stability of our system. We applied Eq. (2) to our nanoemulsions with droplet size less than 100 nm, which have optimal composition of the HLB value (11.1), oil/surfactant weight ratio (0.6) and droplet volume fraction (0.08). As seen in Fig. 4, the value of "$10^5\ r^{-2}$" decreases slightly, implying that coalescence occurs at a slow pace [33]. Second, Ostwald ripening is caused by the difference in solubility between small droplets and different large droplets because of the different Laplace pressures. Lifshitz and Slezov [34] and Wagner [35] independently produced a theory, the so-called LSW theory, for Ostwald ripening of particles. According to the following equation, the rate of Ostwald ripening, ω is

$$\omega = dr^3/dt = 8/9(C_\infty\gamma V_m D)/\rho RT, \tag{3}$$

where r is the average droplet radius, t is the time of storage, C_∞ is the bulk phase solubility, γ is the interfacial tension, V_m is the molar volume of the oil, D is the diffusion coefficient of the oil phase in the continuous phase, ρ is the density of the oil, R is the gas constant, and T is the absolute temperature. Eq. (3) predicts a linear relation between r^3 and t. These linear plots mean that the main driving force for an unstable system is the Ostwald ripening rate [36,37].

The stability of these nanoemulsion systems was assessed by measuring the change in droplet size with storage time at room temperature (~25 °C). The droplet size of nanoemulsions prepared by phase inversion composition at elevated temperatures little changed over the 4-weeks (Fig. 5). This result implies that Ostwald ripening of our nanoemulsion system occurs at a constant speed (Fig. 6).

CONCLUSION

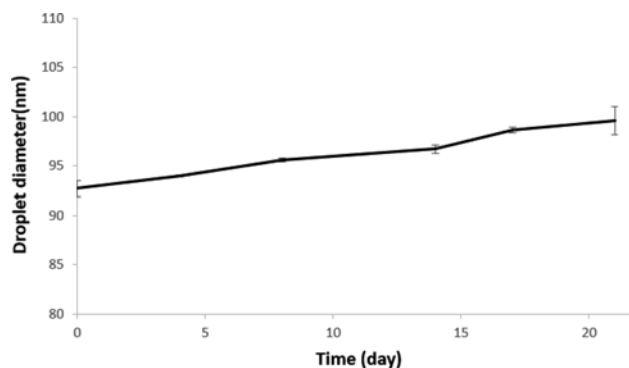Nanoemulsions have been obtained in the hexadecane (C16)/

Fig. 5. The r^3 of nanoemulsion as a function of time for samples with HLB value=11, O/S=0.6, and droplet volume fraction= 0.08.
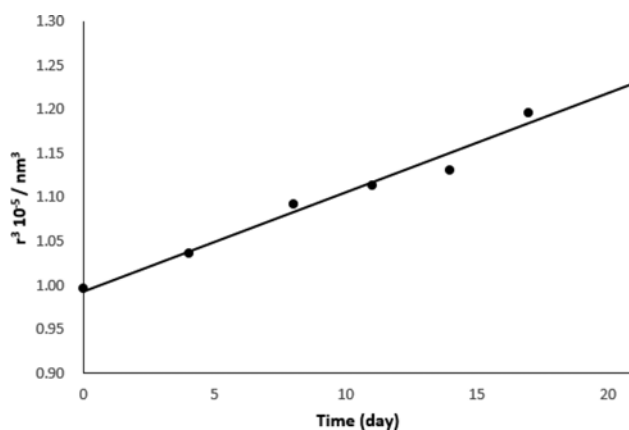

Fig. 6. Droplet diameter as a function of time for samples with HLB value=11, O/S=0.6, and droplet volume fraction=0.08.

surfactant (HCO-60 and Span 80)/water system by phase inversion composition at elevated temperature. A 3 w/w% oil concentration and a 5 w/w% surfactant were used for nanoemulsion formation. The proper HLB value of the surfactants and the structure of surfactant during the emulsification process in the emulsion system was a key factor for minimal droplets. We can confirm the phase inversion point by use of viscosity and conductivity measurements. The stability of the nanoemulsion was confirmed by the droplet size change. The droplet size of the nanoemulsion did not change over the 4-weeks. The PIC method at elevated temperature is an attractive method for preparation of nanoemulsions because this method leads to formation of higher inner phase volume nanoemulsions with long-term stability.

REFERENCES

1. D. J. McClements, E. A. Decker and J. Weiss, *J. Food Sci.*, **72**, 109

(2007).

2. D. J. McClements, *Soft Matter*, **48**, 2279 (2011).

3. O. S. Aubrun, J. T. Simonnet and F. L. Alloret, *Adv. Colloid Interface Sci.*, **108**, 145 (2004).

4. C. Solans, P. Izquierdo, J. Nolla, N. Azemar and M. J. Garcia-Celma, *Curr. Opin. Colloid Interface Sci.*, **10**, 102 (2005).

5. T. Tadros, P. Izquierdo, J. Esquena and C. Solans, *Adv. Colloid Interface Sci.*, **108**, 303 (2004).

6. N. Sadurn, C. Solans, N. Azemara and M. J. Garcia-Celma, *Eur. J. Pharm. Sci.*, **26**, 438 (2005).

7. N. Atrux-Tallau, T. Delmas, S. H. Han, J. W. Kim and J. Bibette, *Int. J. Cosmet. Sci.*, **35**, 310 (2013).

8. P. P. Constantinides, *Pharm. Res.*, **12**, 1561 (1995).

9. L. Yu, C. Li, J. Xu, J. Hao and D. Sun, *Langmuir*, **28**, 14547 (2012).

10. S. M. Jafari, Y. He and B. Bhandari, *Food Res. Int.*, **40**, 862 (2007).

11. S. Kentish, T. J. Wooster, M. Ashokkumar, S. Balachandran, R. Mawson and L. Simons, *Innovative Food Sci. Emerg. Technol.*, **9**, 170 (2008).

12. J. Rao and D. J. McClements, *J. Agric. Food Chem.*, **58**, 7059 (2010).

13. K. Nakabayashi, F. Amemiya, T. Fuchigami, K. Machida, S. Takeda, K. Tamamitsu and M. Atobe, *Chem. Commun.*, **47**, 5765 (2011).

14. S. Graves, K. Meleson, J. Wilking, M. Y. Lin and T. G. Mason, *J. Chem. Phys.*, **122**, 134703 (2005).

15. K. Roger, B. Cabane and U. Olsson, *Langmuir*, **27**, 604 (2011).

16. I. Sole, A. Maestro, C. Gonzalez, C. Solans and J. M. Gutierrez, *Langmuir*, **22**, 8326 (2006).

17. L. Dai, W. Li and X. Hou, *Colloids Surf., A*, **125**, 27 (1997).

18. H. Sagitani, *J. of Korean Oil Chemists' Soc.*, **58**, 738 (1981).

19. C. Solans and I. Sole, *Curr. Opin. Colloid Interface Sci.*, **17**, 246 (2012).

20. J. M. Gutierrez, C. Gonzalez, A. Maestro, I. Sole, C. M. Pey and J. Nolla, *Curr. Opin. Colloid Interface Sci.*, **13**, 245 (2008).

21. A. Forgiarini, J. Esquena, C. Gonzalez and C. Solans, *Langmuir*,

17, 2076 (2001).

22. T. Antonya, A. Saxenaa, K. B. Royb and H. B. Bohidara, *J. Biochem. Biophys. Methods*, **36**, 75 (1998).

23. C. M. Pey, A. Maestro, I. Sole, C. Gonzalez, C. Solans and J. M. Gutierrez, *Colloids Surf., A*, **288**, 144 (2006).

24. W. Liu, D. Sun, C. Li, Q. Liu and J. Xu, *J. Colloid Interface Sci.*, **303**, 557 (2006).

25. P. Fernandez, V. Andre, J. Rieger and A. Kuhnle, *Colloids Surf., A*, **251**, 53 (2004).

26. E. Nazarzadeh, T. Anthonypillai and S. Sajjadi, *J. Colloid Interface Sci.*, **397**, 154 (2013).

27. S. Mayer, J. Weiss and D. J. McClements, *J. Colloid Interface Sci.*, **402**, 122 (2013).

28. J. N. Wilking, C. B. Chang, M. M. Fryd, L. Porcar and T. G. Mason, *Langmuir*, **27**, 5204 (2011).

29. A. R. Malheiro, L. C. Varanda, J. Perez and H. M. Villullas, *Langmuir*, **23**, 11015 (2007).

30. L. B. Lopes, H. Vandewall, H. T. Li, V. Venugopal, H. K. Li, S. Naydin, J. Hosmer, M. Levendusky, H. Zheng, M. Vitoria, L. B. Bentley, R. Levin and M. A. Hass, *J. Pharm. Sci.*, **99**, 1346 (2010).

31. A. Forgiarini, J. Esquena, C. González and C. Solans, *Langmuir*, **17**, 2076 (2001).

32. P. Izquierdo, J. Esquena, T. F. Tadros, C. Dederen, M. J. Garcia, N. Azemar and C. Solans, *Langmuir*, **18**, 26 (2002).

33. B. Deminiere, In *Modern Aspects of Emulsion Science,* B. P. Binks Ed., The Royal Society of Chemistry, Cambridge (1998).

34. I. M. Lifshitz and V. V. Slezov, *J. Phys. Chem. Solids*, **19**, 35 (1961).

35. C. Wagner, *Zeit. Electrochem.*, **65**, 581 (1961).

36. D. Morales, J. M. Gutiérrez, M. J. García-Celma and Y. C. Solans, *Langmuir*, **19**, 7196 (2003).

37. H. J. Yang, W. G. Cho and S. N. Park, *J. Ind. Eng. Chem.*, **15**, 331 (2009).